How to cite: *Angew. Chem. Int. Ed.* **2022,** *61,* e202205371
International Edition: doi.org/10.1002/anie.202205371
German Edition: doi.org/10.1002/ange.202205371

Phosphorus Heterocycles

Bis(imidazolium)-1,3-diphosphete-diide: A Building Block for FeC_2P_2 Complexes and Clusters

Moritz Theodor Scharnhölz, Peter Coburger, Lisa Gravogl, Daniel Klose, Juan José Gamboa-Carballo, Grégoire Le Corre, Jonas Bösken, Clara Schweinzer, Debora Thöny, Zhongshu Li, Karsten Meyer, and Hansjörg Grützmacher**

Dedicated to Professor John Nixon

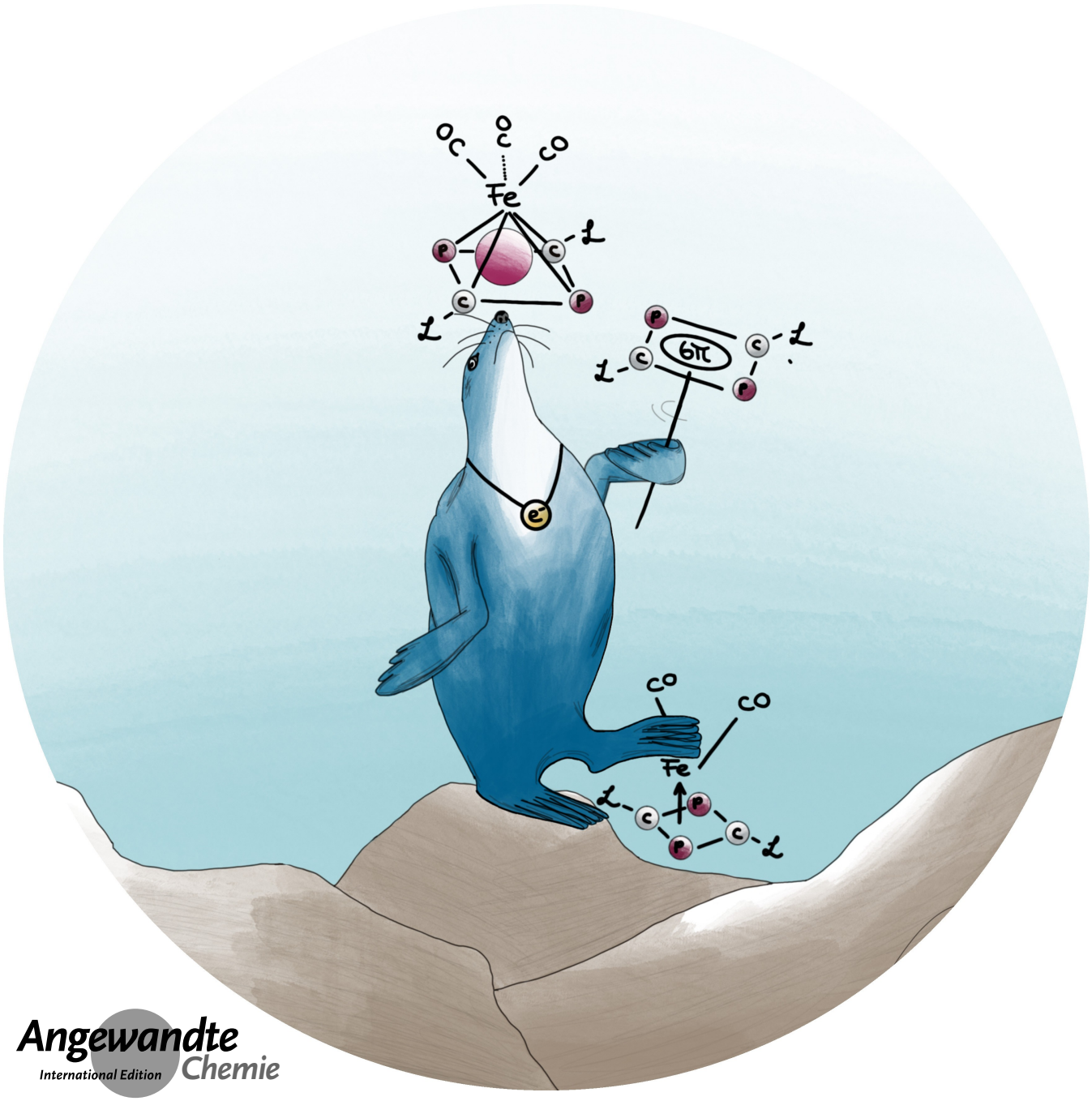

Abstract: Reaction of the 6π-electron aromatic four-membered heterocycle $(IPr)_2C_2P_2$ (**1**) (IPr = 1,3-bis(2,6-diisopropylphenyl)-1,3-dihydro-2*H*-imidazol-2-ylidene) with $[Fe_2CO_9]$ gives the neutral iron tricarbonyl complex $[Fe(CO)_3\text{-}\eta^3\text{-}\{(IPr)_2C_2P_2\}]$ (**2**). Oxidation with two equivalents of the ferrocenium salt, $[Fe(Cp)_2](BArF_{24})$, affords the dicationic tricarbonyl complex $[Fe(CO)_3\text{-}\eta^4\text{-}\{(IPr)_2C_2P_2\}](BArF_{24})_2$ (**4**). The one-electron oxidation proceeds under concomitant loss of one CO ligand to give the paramagnetic dicarbonyl radical cation complex $[Fe(CO)_2\text{-}\eta^4\text{-}\{(IPr)_2C_2P_2\}](BArF_{24})$ (**5**). Reduction of **5** allows the preparation of the neutral dicarbonyl complex $[Fe(CO)_2\text{-}\eta^4\text{-}\{(IPr)_2C_2P_2\}]$ (**6**). An analysis by various spectroscopic techniques (^{57}Fe Mössbauer, EPR) combined with DFT calculations gives insight into differences of the electronic structure within the members of this unique series of iron carbonyl complexes, which can be either described as electron precise or Wade–Mingos clusters.

Introduction

The discovery of ferrocene, $[Fe(Cp)_2]$ = Fc,[1] revolutionized the understanding of the interaction between a transition metal and a cyclic multi-hapto-bound ligand with a conjugated π-electron system.[2] The bonding in ferrocene can be explained with a molecular orbital correlation diagram, in which symmetry-adapted occupied and vacant orbitals at the Fe^{II} center and the Cp^- ligand interact.[3] Alternative descriptions exist,[4] and one of them considers Fc being composed of two *nido*-clusters with the Fe center as vertex-sharing atom.[5] One way to probe the interaction between a metal center and its ligand is to investigate the redox behavior.[6] Mild oxidation agents oxidize Fc to the corresponding mono cation, ferrocenium, Fc^+.[12] Ferrocene derivatives, however, can be converted to the dication[13] or monoanion.[14] All redox events mainly involve the iron center supporting a description, in which an Fe^{n+} (n = 1, 2, 3, 4) ion interacts with two Cp^- rings. Another way to experimentally probe the electronic effect of a ligand L and the electron density at a metal center, is to investigate complexes, which—apart from L—carry carbonyls as co-ligands. A high electron density at the metal center is reflected by a low CO stretching frequency due to M→CO back-bonding.[15] Figure 1 shows selected 18 valence electron (18 VE) configured complexes relevant to this work. The cationic complex $[Fe(CO)_3(Cp)]^+$ (**I**) shows IR vibrational absorption bands at ν_{CO} = 2120, 2068 cm^{-1},[7] (Table 1) indicating rather weak d(Fe)→π*CO back-donation, in accord with the assumption that the iron ion is rather electron poor and has the formal oxidation state +2. Reduction of **I** by two electrons is accompanied by loss of CO and leads to the formally isoelectronic, highly sensitive anionic complex $[Fe(CO)_2(Cp)]^-$ (**II**; 18 VE) (ν_{CO} = 1880, 1845 cm^{-1}; Table 1), where the CO stretching frequencies have been shifted by more than 200 cm^{-1} to lower frequencies with respect to **I** indicating strong d(Fe)→π*CO back-donation.[8] This is also true for neutral highly reactive and rare iron arene complexes such as $[Fe(CO)_2(C_6Me_6)]$ (**III**; 18 VE) with ν_{CO} = 1954, 1892 cm^{-1} (Table 1).[9] In both complexes, **II** and **III**, a formal oxidation state of zero can be assigned to iron. On the contrary, the iron cyclobutadiene tricarbonyl complex $[Fe(CO)_3(C_4H_4)]$ (**IV**; 18 VE),[10] also known as Pettit's reagent, shows stretching frequencies at higher wavenumbers ν_{CO} = 2055, 1985 cm^{-1} (Table 1) indicat-

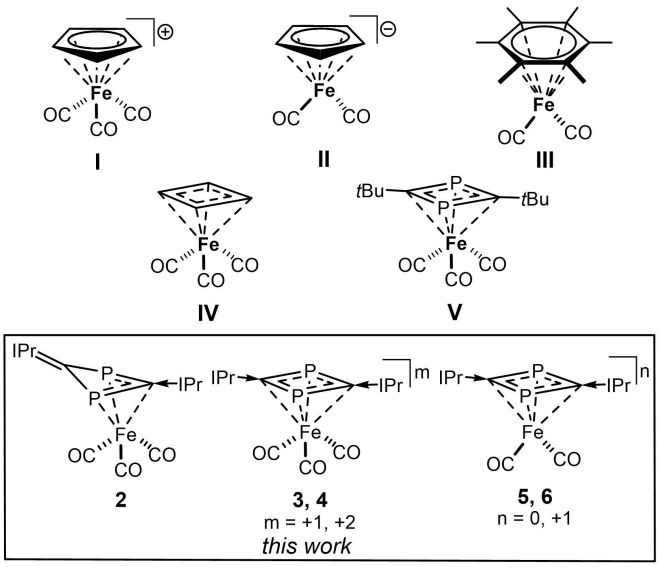

Figure 1. Selected iron carbonyl complexes **I**,[7] **II**,[8] **III**,[9] **IV**,[10] and **V**.[11] Counter anion for all species from this work: $BArF_{24}^-$.

[*] M. T. Scharnhölz, P. Coburger, D. Klose, J. J. Gamboa-Carballo, G. Le Corre, J. Bösken, C. Schweinzer, D. Thöny, H. Grützmacher
Department of Chemistry and Applied Biosciences, ETH Zürich
Vladimir-Prelog-Weg 1, 8093 Zürich (Switzerland)
E-mail: pcoburger@inorg.chem.ethz.ch
hgruetzmacher@ethz.ch
L. Gravogl, K. Meyer
Department of Chemistry and Pharmacy, Inorganic Chemistry, Friedrich-Alexander-Universität Erlangen-Nürnberg (FAU)
Egerlandstr. 1, 91058 Erlangen (Germany)
J. J. Gamboa-Carballo
Higher Institute of Technologies and Applied Sciences (InSTEC), University of Havana
Ave. S. Allende 1110, 10600 Havana (Cuba)
Z. Li
Lehn Institute of Functional Materials (LIFM), School of Chemistry, Sun Yat-Sen University
510275 Guangzhou (China)
and
State Key Laboratory of Elemento-Organic Chemistry, Nankai University
30071 Tianjin (China)

Table 1: Selected analytical data. CO stretching frequencies were measured by ATR-IR. Values marked with a rhombus (♦) were measured by transmission-IR in saturated *n*-hexane solution. Values marked with an asterisk (*) were measured by transmission-IR in acetonitrile solution. Values marked with a dot (●) were measured by transmission-IR in saturated THF solution. For detailed spectra and calculations see the Supporting Information. †: centroid of the coordinated PCP-plane was constructed. Mössbauer and IR data calculated by DFT are given in italics.

Compound	CO-stretch freq. exp. [cm^{-1}]	CO-stretch freq. calc. [cm^{-1}]	C_{Ipr}–C_{ring} bond length [Å]	N–C(–N) bond length [Å]	Fe-centroid distance [Å]	^{57}Fe Mössbauer isomer shift [mms^{-1}]	^{57}Fe Mössbauer quad. splitting [mms^{-1}]
1	–	–	Ø 1.387(3)[23]	Ø 1.375(3)[23]	–	–	–
2	*1983♦, 1917♦, 1904♦	*1976, 1922, 1913*	1.437(5) 1.340(6)	Ø 1.369(4) Ø 1.403(4)	1.909(1)†	0.05 *(−0.03)*	1.14 *(−0.94)*
3	2015*, 1948*	*2018, 1969, 1960*	–	–	–	*– (0.18)*	*– (1.52)*
4	2083,* 2035*	*2070, 2028, 2023*	Ø 1.449(4)	Ø 1.355(3)	1.825(1)	0.11 *(0.02)*	1.40 *(1.24)*
5	1966*, 1903*	*1978, 1930*	Ø 1.432(5)	Ø 1.355(5)	1.804(2)	0.27 *(0.20)*	1.06 *(0.94)*
6	1870, 1807*	*1897, 1850*	Ø 1.409(4)	Ø 1.364(4)	1.776(1)	0.12 *(0.05)*	1.44 *(−1.49)*
I	2120, 2068[7]	*2127, 2083*	–	–	1.710(1)[27]	0.05[28] *(0.07)*	1.88[28] *(1.75)*
II	1881●, 1808●, 1864●, 1770●[8a]	*1875, 1819*	–	–	1.7284(15)[29]	*(0.26)*	*(−2.76)*
III	1954, 1892[9]	*1970, 1920*	–	–	–	*(0.22)*	*(−1.89)*
IV	2055, 1985[10]	*2049, 1991, 1986*	–	–	1.770(1)[30]	0.02[31] *(0.00)*	1.54[31] *(1.52)*
V	–	*2040, 1992, 1982*	–	–	–	*(0.00)*	*(1.14)*

ing that the—in unbound form anti-aromatic—C_4H_4 ring is a rather weak electron donor. Neutral **IV** decomposes upon oxidation under loss of C_4H_4[16] but bulky electron-donating substituents in the ring, which lower ν_{CO} up to 30 cm^{-1}, allow to stabilize the oxidized products.[17]

Sandwich complexes with π-conjugated heterocycles, in which a CR unit has been replaced by a phosphorus center—a research area fueled by the diagonal relationship between carbon and phosphorus[18]—have been widely studied.[19] While iron complexes with η^6-bound six-membered rings $(CR)_{6-x}P_x$ are relatively rare,[20] those with five-membered η^5-bound phospholide rings $(CR)_{5-x}P_x$ are numerous.[19,21]

Often, anodic (positive) shifts of the redox potential were observed[21b] and the overall conclusion is that replacement of a CR unit by phosphorus decreases the σ-electron donating properties of the heterocycle while the π-accepting properties increase strongly.[21c] It is assumed that the redox processes take place mainly at the iron center.[19] Iron complexes with π-conjugated four-membered rings, such as 1-, 1,2- and 1,3-diphosphacyclobutadienes or even $[P_4]^{2-}$ as ligands, are known[22] but few like the complex $[Fe(CO)_3$-η^4-$(t\mathrm{Bu}_2C_2P_2)]$ **V**,[11] related to Pettit's reagent **IV**, contain carbonyls as co-ligands. The calculated ν_{CO} = 2040, 1992, 1982 cm^{-1} of **V** (Table 1) are quite similar to **IV**; thus, indicating rather weak M→CO back-donation.

The recently reported $(IPr)_2C_2P_2$ (**1**) can be considered as an N-heterocyclic carbene stabilized cyclic "dicarbondiphosphide" **A** or, more appropriately, as a bis(imidazolium)-1,3-diphosphete-diide **B** with a formal 2− charge in the C_2P_2 ring and positive charges on every IPr (IPr = 1,3-bis(2,6-diisopropylphenyl)-1,3-dihydro-2*H*-imidazol-2-ylidene) unit. Both descriptions lead to a central aromatic 6π-electron system delocalized over the C_2P_2 ring. Heterocycle **1** is easily oxidized at $E^\circ = -0.451$ V (vs. Fc/Fc^+) to its persistent radical cation[23] and binds to $M(CO)_3$ fragments (M = Cr, Mo) as electron donating ligand.[24]

Here, we report that **1** not only allows to prepare neutral iron dicarbonyl complexes, which—in contrast to arene complexes—are remarkably stable but also show a rich redox chemistry. Specifically, a comparison between $[Fe(CO)_3$-η^4-$\{(IPr)_2C_2P_2\}]^{2+}$ and $[Fe(CO)_2$-η^4-$\{(IPr)_2C_2P_2\}]$ will show that subtle differences in the structure may lead to significant differences in the electronic structure of the central FeC_2P_2 core.

Results and Discussion

Heterocycle **1** reacted with $[Fe_2CO_9]$ in mesitylene at 130 °C to give $[Fe(CO)_3\{\eta^3$-$(IPr)_2C_2P_2\}]$ **2** in two hours (Scheme 1). The product is isolated as dark blue powder (73 % yield), which always contained a second, minor species (≤5 %; $[\delta(^{31}P\{^1H\}) = \delta = 18.2$ ppm (Fe*P*); $\delta = -98.6$ ppm (*P*), $^2J_{PP} = 15$ Hz)]) that could not be further characterized (for details see the Supporting Information, Figures S1–S4). The major compound **2** shows one broadened ^{31}P NMR resonance $[\delta(^{31}P\{^1H\}) = 79.2$ ppm; $\Delta\nu^{1/2} = 85$ Hz] indicating hindered rotation of the $Fe(CO)_3$ moiety (for variable temperature NMR spectra and solid-state NMR spectra see the Supporting Information, Figures S6–S8). A single crystal of **2** could be obtained and allowed to determine the structure by X-ray diffraction methods (see below). Cyclic voltammetry (CV) of solutions of **2** in THF (containing 0.1 M $(n\mathrm{Bu}_4N)PF_6$ as electrolyte; scan rate: 100 mV s^{-1}) showed two quasi-reversible redox waves at −0.83 V and −1.18 V vs. Fc/Fc^+ (Figure S11). Chemical oxidation of **2** with two equivalents of $Fc[BArF_{24}]$ ($BArF_{24}$ = tetrakis[3,5-bis(trifluoromethyl)-phenyl]borate) in 1,2-difluorobenzene (DFB) gave the dicationic tricarbonyl complex $[Fe(CO)_3\{\eta^4$-$(IPr)_2C_2P_2\}](BArF_{24})_2$ (**4**) $[\delta(^{31}P\{^1H\}) = 57.1$ ppm], which is obtained after recrystallization from 1,2-DFB/*n*-hexane as analytically pure, golden crystals (Scheme 1). From the separation of the two redox waves by $\Delta\Delta E = 0.35$ V a small equilibrium constant of K_{disp} =

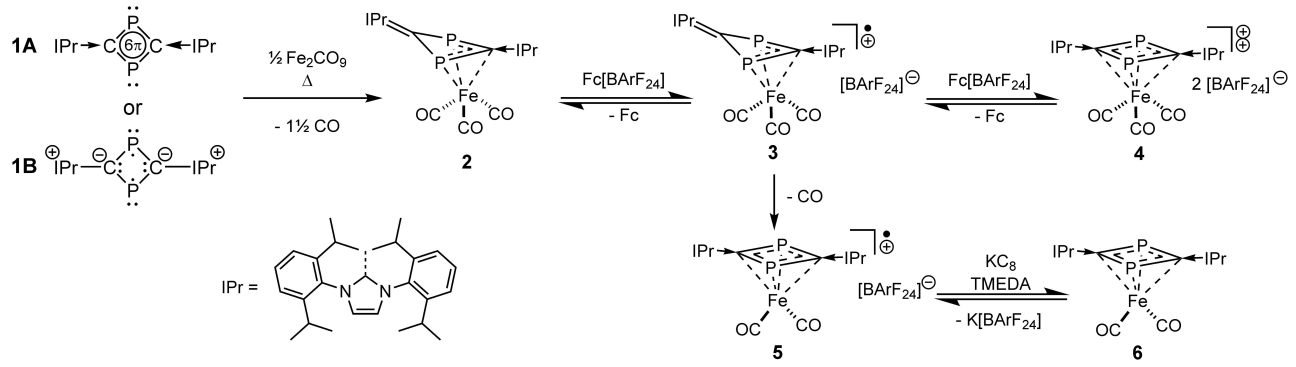

Scheme 1. Possible descriptions of **1** as (A) and (B). Reaction of ligand **1** with $[Fe_2(CO)_9]$ provides complex **2**. Oxidation of **2** with $Fc(BArF_{24})$ ($BArF_{24}$ = tetrakis[3,5-bis(trifluoro-methyl)phenyl]borate) yields Fe^{I} complex **3**. Radical cation **3** either loses CO leading to the formation of radical cation **5**, or can be oxidized a second time by one electron under formation of **4**. Reduction of **5** with KC_8/TMEDA leads to formation of the neutral dicarbonyl complex **6**.

1.24×10^{-6} for the disproportionation of the one-electron oxidation product $[Fe(CO)_3\{\eta^3\text{-}(IPr)_2C_2P_2\}]^{\bullet+}$ (**3**) into **2** and **4** is calculated suggesting that the radical cation **3** may be observed at least spectroscopically. Indeed, mixing of equimolar amounts of **2** and **4** in a polar solvent (fluorobenzene, 1,2-DFB, or acetonitrile) resulted in the immediate formation of a new species **3** (Scheme 1), which is NMR-silent but is characterized by two new absorptions at $\nu_{CO}=2015$ and 1948 cm^{-1} in the IR spectrum. Furthermore, an EPR spectrum was recorded (see below and Figures S16 and S17 in the Supporting Information). Complex **3** is a transient species that loses CO with a half-life of about $\tau_{1/2}\approx4$ h to form the stable iron dicarbonyl radical cation $[Fe(CO)_2\{\eta^4\text{-}(IPr)_2C_2P_2\}]^{\bullet+}$ ($BArF_{24}$) (**5**) (Scheme 1). The CV of a solution of **5** in THF [0.1 M (nBu$_4$N)PF_6 as electrolyte; scan rate: 100 mV s^{-1}] shows a quasi-reversible redox wave at a potential of −1.29 V vs. Fc/Fc^+ (for details see the Supporting Information, Figure S26). Reduction of **5** with KC_8 in a mixture of *n*-hexane/TMEDA (TMEDA = *N*,*N*,*N*′,*N*′-tetramethyl-ethane-1,2-diamine) gave the neutral dicarbonyl compound **6** (Scheme 1).[25] Note that **6** could not be obtained by thermal or photochemical removal of CO from the tricarbonyl complex **2** (see Figure S9 in the Supporting Information for TGA-MS-IR spectra) in agreement with DFT calculations, which indicate that CO loss from **2** is strongly endergonic ($\Delta G=18.7$ kcal mol^{-1}) while CO dissociation from **3** ($\Delta G=-1.4$ kcal mol^{-1}) is slightly exergonic. The lowering of the CO binding energy by as much as 20.1 kcal mol^{-1} is a consequence of the reduced d(Fe)→π*CO back-bonding in the radical cation **3**. The $^{31}P\{^1H\}$ NMR spectra of complexes **4** [$\delta(^{31}P\{^1H\})=58.3$ ppm] and **6** [$\delta(^{31}P\{^1H\})=48.5$ ppm] show a singlet resonance in the range also observed for $[Cr(CO)_3\{\eta^4\text{-}(IPr)_2C_2P_2\}]$ [$\delta(^{31}P)=64.7$ ppm] and $[Co(CO)_2\{\eta^4\text{-}(IPr)_2C_2P_2\}]^+$ [$\delta(^{31}P)=66.3$ ppm], in which the C_2P_2 ring is symmetrically η^4-coordinated.

Single crystals for X-ray diffraction analysis could be obtained for the iron complexes **2**, **4**, **5**, and **6**. In **2**, ligand **1** coordinates to the $Fe(CO)_3$ fragment in an η^3-fashion via the two phosphorus atoms and one carbon atom of the central C_2P_2 ring (Figure 2A). The exocyclic C1–C6 bond [1.340 (6) Å] is significantly shorter than the C2–C7 bond [1.437 (5) Å]; thus, indicating that the IPr unit bound to C2 is best described as an imidazolium group and the coordinated PCP unit serves as 4π-electron donor comparable to an allyl ligand. This assignment is supported by DFT calculations, which indicate a formal double bond between C1 and C6 and a single bond between C2 and C7 (see the Supporting Information). The C_2P_2 ring is not planar but adopts a butterfly conformation [fold angle along the P–P axis 25.2(3)°]. In complexes **4** (Figure 2B), **5** (Figure 2C), and **6** (Figure 2D), the central C_2P_2 ring is η^4-coordinated to the iron centers. The C_{Ipr}–C_{ring} bonds between the IPr moieties and the central C_2P_2 ring are rather long [**4**: 1.449(4) Å, **5**: 1.432(5) Å, **6**: 1.409(4) Å] indicating imidazolium character of the IPr units and, in return, electron donation into the C_2P_2 ring. As expected, the distance between the iron center and the ring centroid (ct), Fe–ct, is shorter in **4** [1.825(1) Å], **5** [1.804(2) Å], and **6** [1.776(1) Å] in comparison to the Cr complex $[Cr(CO)_3\{\eta^4\text{-}(IPr)_2C_2P_2\}]$ (Cr–ct = 1.929(1) Å]. The Co–ct bond in $[Co(CO)_2\{\eta^4\text{-}(IPr)_2C_2P_2\}]^+$ (Co–ct = 1.806 (1) Å] shows a similar length. A shortening of the Fe–ct bond in going from the tricarbonyl complex **4** to the dicarbonyl complex **5** can be ascribed to the loss of a CO ligand (although this effect is certainly counter-balanced by decreasing the formal charge from +2 to +1). The even shorter Fe–ct bond in neutral **6**, however, is astonishing given that **6** was generated from **5** by one-electron reduction.

The stretching frequencies, ν_{CO}, of the CO groups follow the expected trends (Table 1). In the tricarbonyl complexes **2**, **3**, and **4**, the increasing positive charge correlates with increasing stretching frequencies due to diminished d(Fe)→π*CO orbital back-bonding. The opposite is observed when the dicarbonyl radical cation **5** ($\nu_{CO}=1970$, 1908 cm^{-1}) is reduced to the neutral complex **6** ($\nu_{CO}=1870$, 1807 cm^{-1}). Note that—with the exception of dicationic **4**—the ν_{CO} are observed at significantly lower wavenumbers than in comparable iron tricarbonyl complexes with conjugated cyclic hydrocarbons as ligands, such as Cp^- in **I** or C_4H_4 in **III**. Also, $[Fe(CO)_3(t\text{Bu}_2C_2P_2)]$ **IV** ($\nu_{CO}=2040$, 1990 cm^{-1}) has

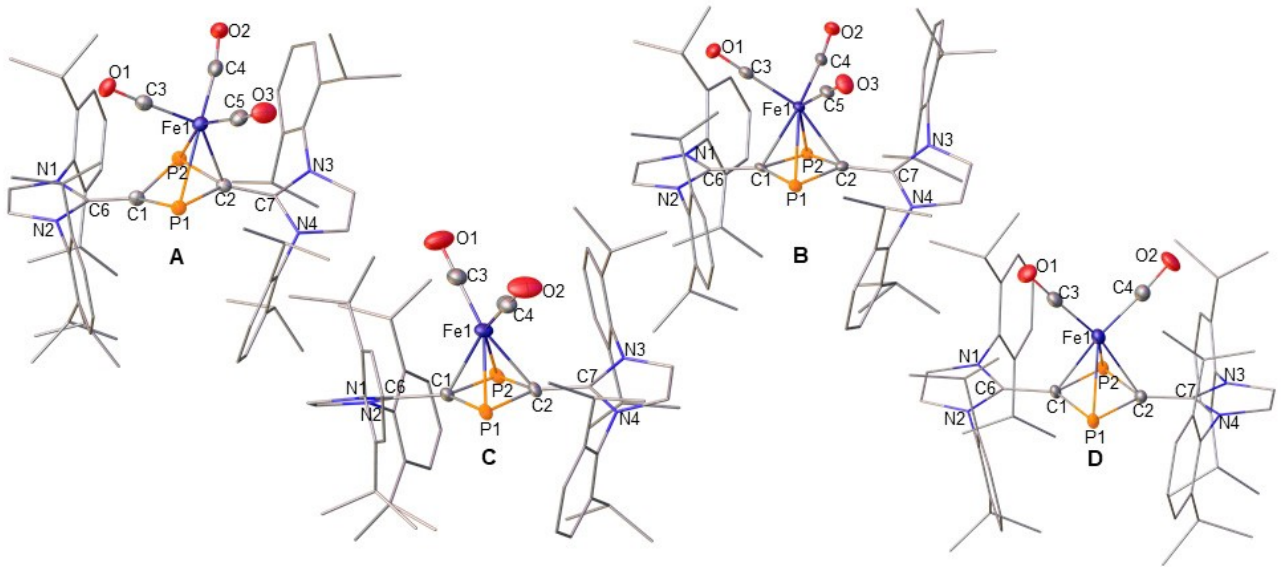

Figure 2. Solid-state structures of iron complexes **2** (A), **4** (B), **5** (C), and **6** (D). Hydrogen atoms, counter ions and solvent molecules are omitted for clarity. Selected metrical parameters can be found in Table 1.[26]

higher ν_{CO} stretching frequencies than all complexes with **1** as ligand. The same trend is observed when the dicarbonyl complexes $[Fe(CO)_2(C_6Me_6)]$ **II** and $[Fe(CO)_2$-η^4-$\{(IPr)_2C_2P_2\}]$ **6** are compared. The latter complex shows the lowest stretching frequencies of all complexes reported here; indicating especially strong electron donation of $(IPr)_2C_2P_2$ **1** to the $Fe(CO)_2$ unit. Only the anionic complex $[Fe(CO)_2(Cp)]^-$ shows similar low stretching frequencies (see above and Table 1).[8] The paramagnetic complexes $[Fe(CO)_3\{\eta^3$-$(IPr)_2C_2P_2\}]^{\bullet+}$ (**3**) and $[Fe(CO)_2\{\eta^4$-$(IPr)_2C_2P_2\}]^{\bullet+}$ (**5**) were further investigated by EPR spectroscopy in frozen fluorobenzene/toluene solution (1:1 mixture). For **3**, an axial g-tensor with the principal values $g_x = g_y = 2.0166$ and $g_z = 1.9858$ ($g_{iso} = 2.0062$) was obtained (Figure 3A and Figure S17). Complex **5** also shows an axial g-tensor, however, the g-values ($g_x = g_y = 2.1287$, $g_z = 2.0021$, $g_{iso} = 2.0865$) are larger compared to **3** and g_{iso} deviates more strongly from the free-electron value ($g = 2.0023$) indicating a larger spin-

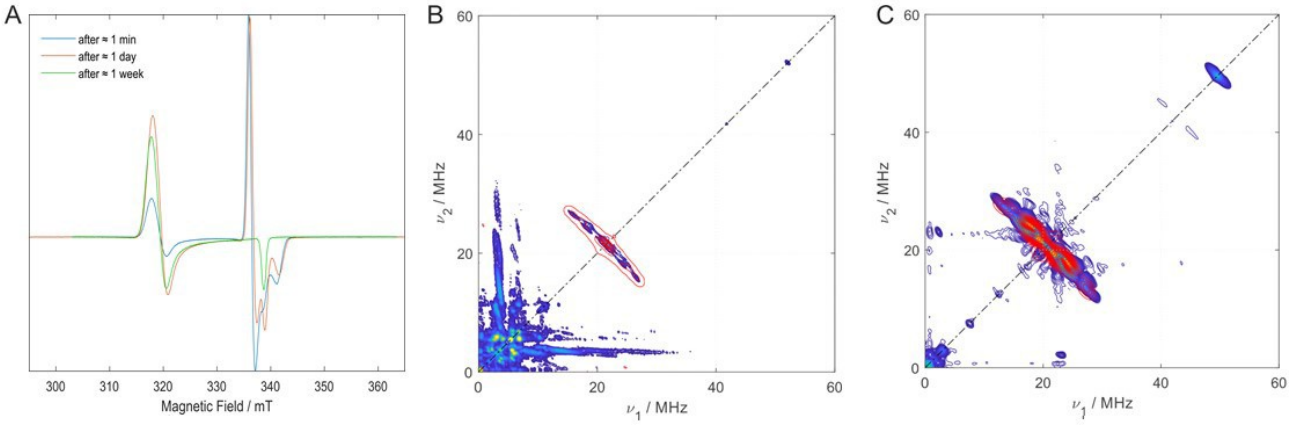

Figure 3. EPR spectra and ^{31}P hyperfine couplings of **3** and **5**. A) Reaction of **3** to **5** as monitored by cw EPR. (ca. 9.5 GHz, 20 K, frozen solution). Blue spectrum: after ≈ 1 min, red spectrum after ≈ 1 day, green spectrum after ≈ one week. Note that the final spectrum (green) shows a single spectral component and thereby allows for an unambiguous resonance assignment and g-tensor determination. HYSCORE spectra (ca. 34.4 GHz) of **3** (B) and **5** (C) in blue/yellow obtained at the spectral maximum of the respective component and simulations (red). Both spectra show clear ridges due to ^{31}P couplings centered around the ^{31}P nuclear Zeeman frequency of 20 and 21 MHz in (B) and (C), respectively. The simulated ^{31}P hyperfine coupling (HFC) tensors (red) are (4.4, 3.2, 1.5) MHz, (1.6, 5.5, 3.0) MHz in **3** and (−8.0, 7.4, 1.7) MHz, (−0.5, 5.8, 1.0) MHz in **5**. Due to their initial low modulation depth, ^{31}P nuclear frequencies were enhanced by matching pulses in **C** (see the Supporting Information). The calculated ^{31}P HFC values [**3**: (−21.8, 12.6, −12.3) MHz, (−11.1, 1.5, 12.0) MHz; **5**: (7.7, 16.4, −23.0) MHz, (27.0, 16.0, −20.2) MHz] deviate from the experimental ones but the symmetry of the tensors is reproduced. The two different sets of ^{31}P HFCs result from hindered rotation of the $Fe(CO)_3$ or $Fe(CO)_2$ units in **3** and **5**, respectively.

density on the iron center in **5**. The pulse EPR technique HYSCORE,[32] allows to determine ^{31}P hyperfine couplings (HFC's) in the two complexes. Because of the hindered rotation of the $Fe(CO)_3$ or $Fe(CO)_2$ units in **3** and **5**, respectively, in frozen solution the complexes become unsymmetric and therefore show two sets of ^{31}P HFCs (Figure 3B, C and Figure S16). The g-tensors obtained from DFT calculations [**3**: $g_{11}=1.9906$, $g_{22}=2.0158$, $g_{33}=2.01890$ ($g_{iso}=2.0084$); **5**: $g_{11}=2.0038$, $g_{22}=2.0087$, $g_{33}=2.1045$ ($g_{iso}=2.0653$)] are in reasonable agreement with the experimental data and validate the electronic structure models. Specifically, that **3** contains a η^3-bound $(IPr)_2C_2P_2$ ligand (like in **2**) and is a 17 VE complex. The spin-population in **3** is distributed over the iron center, the non-coordinating carbon atom of the C_2P_2 ring and the nitrogen atoms of the respective IPr moiety (Fe 0.63, P −0.02 and −0.03, N 0.1 each, C 0.27). For **5**, likewise a 17 VE complex but with a η^4-bound $(IPr)_2C_2P_2$ ligand, a significantly greater spin-density is located on Fe [Fe 1.27, P −0.03 each, N < 0.01, C in C_2P_2 < 0.01], which is in agreement with the larger experimental g_{iso} value. These data suggest that the oxidation from **2** to **3** does not take place solely at the iron center but rather involves the whole complex indicating that $(IPr)_2C_2P_2$ **1** behaves as a redox non-innocent ligand. In contrast, in the redox pair **5**/**6**, the redox event solely takes place at the iron center and **1** acts as a non-redox active innocent ligand in this case.

Zero-field ^{57}Fe Mössbauer spectra were recorded for solid samples of the $(IPr)_2C_2P_2$ complexes **2**, **4**, **5**, and **6** at 77 K (see the spectrum of **6** in Figure 4 as example) and the calculated ^{57}Fe Mössbauer parameters are in good agreement with the experimental data (Table 1). For comparison, the experimental and/or calculated data for the complexes with cyclic hydrocarbon ligands (**I–IV**) and $[Fe(CO)_3(tBu_2C_2P_2)]$ **V** were added in Table 1. Despite the significant differences with respect to structure and charge, all complexes—with the exception of **5**—have rather similar ^{57}Fe Mössbauer parameters. Unfortunately, the range of isomer shifts, δ, for these complexes lies within the ones typically observed for both Fe^0 and Fe^{II} low-spin complexes[33] and suggests similar physical oxidation states (electron densities) at the iron centers. The relatively high local symmetry of most complexes—with the exception of **II** (local C_s symmetry)—is reflected by a quadrupole splitting $\Delta E_Q < 2\ mms^{-1}$. The isomer shift $\delta = 0.27\ mms^{-1}$ of the paramagnetic complex $[Fe(CO)_2\{\eta^4\text{-}(IPr)_2C_2P_2\}](BArF_{24})$ (**5**), with its 17-valence electron configuration at the iron center, reflects the deviation from a closed-shell Fe^0 or Fe^{II} (S = 0) compound to a one-electron oxidized species with S = 1/2.

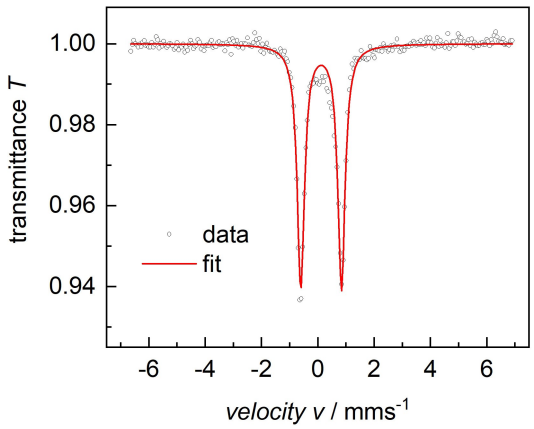

Figure 4. Zero-field ^{57}Fe Mössbauer spectrum of a solid sample of **6** at 77 K. The measured data (circles) were fitted using least-square fitting of the Lorentzian signals (red line).

A comparison of the electronic structure between the dicationic iron tri(carbonyl) complex $[Fe(CO)_3\{\eta^4\text{-}(IPr)_2C_2P_2\}]^{2+}$ (**4**) and the neutral dicarbonyl complex $[Fe(CO)_2\{\eta^4\text{-}(IPr)_2C_2P_2\}]$ (**6**) is especially intriguing (a detailed bonding analysis of the tricarbonyl complex $[Fe(CO)_3\{\eta^3\text{-}(IPr)_2C_2P_2\}]$ (**2**), which is related to $[Fe(CO)_3(\eta^4\text{-arene})]$ complexes will be published elsewhere). Both, **4** and **6**, have the same valence electron (VE) count of 34 within the central FeC_2P_2 core under the assumption that each IPr is bound via a dative two-electron bond to the C_2P_2 ring.[23] **4**: VE = 8(Fe) + 18(C_2P_2) + 4(2 IPr) + 6(3 CO) − 2 (positive charge) = 34; **6**: VE = 8(Fe) + 18(C_2P_2) + 4(2 × IPr) + 4 (2 CO) = 34. The polyhedral skeletal electron pair theory (PSEP), formulated by Wade and Mingos,[34] predicts that the dicationic tricarbonyl complex **4** can be described as a *nido*-cluster, in which 14 e = 7 electron pairs of the total of 34 VE's are used for bonding within the FeC_2P_2 core. On the other hand, the dicarbonyl complex **6** fulfills the EAN rule for electron precise clusters [$b = {}^1/_2(18n + 8m) - VE = {}^1/_2(18 + 32) - 34) = 8$; n = number of transition metal centers; m = number of main group element centers; b = number of 2-center-2-electron-shared bonds within the $m+n$ cluster core]. Consequently, **6** can be viewed as a square pyramidal electron precise FeC_2P_2 cluster, in which every edge corresponds to an electron-shared, 2-center-2-electron (2c2e) bond.

In order to verify this assessment, the wave functions of **4**, and **6** were analyzed by means of intrinsic bond orbitals (IBO)[35] and their localized-orbital centroids (LOCs),[36] using the ORCA program package.[37]

The IBO calculations for **4** show three filled non-bonding 3d orbitals at Fe and three bonding orbitals describing the interaction between the iron center and the η^4-bound C_2P_2 ring (see Figure 5A). One of these orbitals shows an LOC in between the Fe and C_2P_2 ring that accounts for a delocalized covalent P–Fe–P interaction; thus, making a clear assignment of an oxidation state to the iron center in **4** difficult. The other two LOCs are closer to the carbon centers and can be interpreted as localized dative Fe←C bonds (for details see the Supporting Information, Figure S29). This is in accord with the description of **4** as five-vertex *nido*-cluster with a square pyramidal structure, where from the $n+2=7$ skeletal electron pairs three are used for bonding between the Fe center and the C_2P_2 ring (shown as light-blue dots) and four between the C and P centers (these LOCs are indicated by green dots). The NICS (nucleus-independent chemical shift) value at the center of the FeC_2P_2 pyramid in **4** is −32.9 indicating the presence of spherical aromaticity.

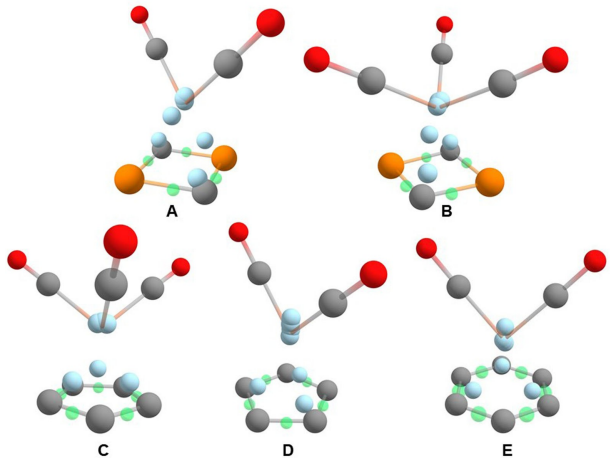

Figure 5. Localised orbital centroids (LOCs) for substances **4** (A), **6** (B), **I** (C), **II** (D), and **III** (E). For detailed calculation results see the Supporting Information, section 3.2. Note that a truncated model was used for **III** where the methyl groups were replaced by hydrogen atoms.

The electronic structure of the dicarbonyl complex **6** is different when compared to **4**. Three non-bonding 3d orbitals are located at the iron center and three orbitals accounting for dative ligand-to-metal donation, Fe←C_2P_2, are found with LOCs strongly located towards the C_2P_2 plane (see Figure 5B). In addition, one LOC lies close to the Fe center and originates from a filled 3d orbital, which is strongly involved in π-back-bonding to the LUMO of the C_2P_2 moiety (see the Supporting Information, section 3.2). As a result, $(IPr)_2C_2P_2$ (**1**) does not only serve as a strong 6π-donor ligand but also as a π-accepting ligand in **6**. These acceptor properties are enabled by the relatively small HOMO–LUMO gap of 2.4 eV in **1**. Furthermore, the LUMO of $(IPr)_2C_2P_2$ (**1**) exhibits C_{Ipr}–C_{ring} bonding character and partial occupation of this orbital by electron back-donation leads to a shortening of these bonds. This specific back-bonding interaction is absent in the dication **4**, explaining the initially surprising lengthening of the Fe–ct distance in **4** compared to **6** (see above). This different electronic structure of **6** results in a lower spherical aromaticity compared to **4**, reflected by a lower NICS value of −20.0 in the center of the C_2P_2Fe pyramid. We propose therefore to describe the dicarbonyl complex **6** as an electron-precise "classical" organometallic complex between an Fe^0 center to which the $(IPr)_2C_2P_2$ ring acts prevalently as a π-donor ligand.

For comparison, we also inspected the iron complexes **I** (Figure 5C), **II** (Figure 5D), and **III** (Figure 5E) carrying either a Cp^- ring or benzene as 6π-aromatic ligand using the same theoretical approach. Clearly, the three LOCs close to the carbon centers characterize these ligands as classical π-electron donor ligands,[4] while three (**I**), respectively, four (**II**, **III**) LOCs at the Fe center indicate Fe^{II} or Fe^0 oxidation states in **I** or **II**, **III**.

Finally, the reaction energies ΔE_r for the ligand exchange reactions (1) and (2) where calculated in order to evaluate the binding energies of $(IPr)_2C_2P_2$ using the neutral dicarbonyl complex **6** as specific example:

$$[Fe(CO)_2(C_6H_6)]\ (\mathbf{III}) + (IPr)_2C_2P_2\ (\mathbf{1}) \rightarrow [Fe(CO)_2\{\eta^4\text{-}(IPr)_2C_2P_2\}]\ (\mathbf{6}) + C_6H_6, \quad \Delta E_r = -27.3\ \text{kcal mol}^{-1} \tag{1}$$

$$[Fe(CO)_2(Cp)]^-\ (\mathbf{II}) + (IPr)_2C_2P_2\ (\mathbf{1}) \rightarrow [Fe(CO)_2\{\eta^4\text{-}(IPr)_2C_2P_2\}]\ (\mathbf{6}) + Cp^-, \quad \Delta E_r = 3.3\ \text{kcal mol}^{-1} \tag{2}$$

The interaction between the $Fe(CO)_2$ fragment and the η^4-bound $(IPr)_2C_2P_2$ ligand in **6** is about 30 kcal mol^{-1} stronger than the iron η^6-benzene bond in complex **III** and about as strong as the interaction between the η^5-cyclopentadienide anion and Fe in complex **II**. These data clearly indicate that $(IPr)_2C_2P_2$ may bind very tightly to transition metal fragments.

Conclusion

The following conclusions can be drawn from the series of iron carbonyl complexes with $(IPr)_2C_2P_2$ (**1**) as ligand: a) The molecule **1** acts as an unusually strong electron donating ligand. This is in contrast to other phosphorus containing heterocycles, which are often referred to as electron accepting ligands. b) As ligand, **1** is electronically remarkably flexible, which relates this compound to redox non-innocent ligands.[6,38] c) The very similar ^{57}Fe Mössbauer isomer shifts δ indicate that the iron nuclei in **4** and **6** must be located in rather similar electronic environments. Regardless, while neutral $[Fe(CO)_3\{\eta^4\text{-}(IPr)_2C_2P_2\}]$ **6** can be viewed as a classical coordination compound with iron in its oxidation state zero, the dication $[Fe(CO)_2\{\eta^4\text{-}(IPr)_3C_2P_2\}]^{2+}$ in **4** is better described as square pyramidal *nido*-cluster, where the oxidation state at the iron center remains uncertain due to the more covalent character of the bonds within the $Fe_2C_2P_2$ core. This is reflected in the experimental data: Reduction of **4** involves the whole FeC_2P_2 core and leads to the expected opening of the cluster structure to give **3**, in which the binding mode of **1** is reduced from η^4 to η^3. d) The use of **1** as ligand opens the possibility to prepare electron-rich neutral iron complexes with cyclic conjugated 6π-aromatic ligands that are significantly more stable than related iron arene complexes.

Acknowledgements

This work was supported by the Swiss National Science Foundation (SNF; grant 2-77199-18) and the ETH Zürich (grant 0-20406-18). PC gratefully acknowledges funding by the Deutsche Forschungsgemeinschaft (DFG, grant 438203135). K.M. thanks the Friedrich-Alexander-Universität Erlangen-Nürnberg (FAU) for generous financial support and H.G. thanks FAU for the participation in the FAU

Visiting Professorship programme. We thank Dr. M. Wöhrle for valuable assistance with the X-ray diffraction measurements and Dr. R. Verel for valuable help with acquisition and interpretation of NMR data. Open Access funding provided by Eidgenössische Technische Hochschule Zürich.

Conflict of Interest

The authors declare no conflict of interest.

Data Availability Statement

The data that support the findings of this study are available from the corresponding author upon reasonable request.

Keywords: Cluster Compounds · Density Functional Calculations · Donor–Acceptor Systems · Iron · Phosphorus

[1] a) T. J. Kealy, P. L. Pauson, *Nature* **1951**, *168*, 1039–1040; b) S. A. Miller, J. A. Tebboth, J. F. Tremaine, *J. Chem. Soc.* **1952**, 632–635.
[2] J. Okuda, *Eur. J. Inorg. Chem.* **2017**, 217–219.
[3] M. J. Mayor-López, J. Weber, *Chem. Phys. Lett.* **1997**, *281*, 226–232.
[4] V. M. Rayón, G. Frenking, *Organometallics* **2003**, *22*, 3304–3308.
[5] E. D. Jemmis, M. M. Balakrishnarajan, P. D. Pancharatna, *J. Am. Chem. Soc.* **2001**, *123*, 4313–4323.
[6] B. de Bruin, P. Gualco, N. D. Paul, *Ligand Design in Metal Chemistry: Reactivity and Catalysis*, Wiley, Hoboken, **2016**, pp. 176–204.
[7] L. Busetto, R. J. Angelici, *Inorg. Chim. Acta* **1968**, *2*, 386–390.
[8] a) A. F. Clifford, A. K. Mukherjee, *J. Inorg. Nucl. Chem.* **1963**, *25*, 1065–1066; b) M. E. Giuseppetti, A. R. Cutler, *Organometallics* **1987**, *6*, 970–973; c) J. E. Ellis, E. A. Flom, *J. Organomet. Chem.* **1975**, *99*, 263–268.
[9] S. R. Weber, H. H. Brintzinger, *J. Organomet. Chem.* **1977**, *127*, 45–54.
[10] G. F. Emerson, L. Watts, R. Pettit, *J. Am. Chem. Soc.* **1965**, *87*, 131–133.
[11] P. Binger, B. Biedenbach, R. Schneider, M. Regitz, *Synthesis* **1989**, *1989*, 960–961.
[12] R. B. Woodward, M. Rosenblum, M. C. Whiting, *J. Am. Chem. Soc.* **1952**, *74*, 3458–3459.
[13] M. Malischewski, M. Adelhardt, J. Sutter, K. Meyer, K. Seppelt, *Science* **2016**, *353*, 678–682.
[14] a) M. G. Walawalkar, P. Pandey, R. Murugavel, *Angew. Chem. Int. Ed.* **2021**, *60*, 12632–12635; *Angew. Chem.* **2021**, *133*, 12740–12743; b) C. A. P. Goodwin, M. J. Giansiracusa, S. M. Greer, H. M. Nicholas, P. Evans, M. Vonci, S. Hill, N. F. Chilton, D. P. Mills, *Nat. Chem.* **2021**, *13*, 243–248.
[15] a) C. Eschenbroich, *Organometallchemie*, 6. ed., Teubner, Leibzig, **2008**; b) C. Eschenbroich, *Organometallics*, 3. ed., Wiley-VCH, Weinheim, **2016**.
[16] a) W. A. Donaldson, *Encyclopedia of Reagents for Organic Synthesis*, Wiley, Hoboken, **2001**; b) R. P. Johnson, *The Chemistry of Cyclobutanes*, Wiley, Hoboken, **2005**, pp. 589–616.
[17] S. Minegishi, K. Komatsu, T. Kitagawa, *Organometallics* **2011**, *30*, 1002–1007.
[18] K. B. Dillon, F. Mathey, J. F. Nixon, *Phosphorus: The Carbon Copy*, Wiley, New York, **1998**.
[19] R. Bartsch, S. Datsenko, N. V. Ignatiev, C. Müller, J. F. Nixon, C. J. Pickett, *J. Organomet. Chem.* **1997**, *529*, 375–378.
[20] a) B. Rezaei Rad, U. Chakraborty, B. Mühldorf, J. A. W. Sklorz, M. Bodensteiner, C. Müller, R. Wolf, *Organometallics* **2015**, *34*, 622–635, and references therein; b) D. Böhm, F. Knoch, S. Kummer, U. Schmidt, U. Zenneck, *Angew. Chem. Int. Ed. Engl.* **1995**, *34*, 198–201; *Angew. Chem.* **1995**, *107*, 251–254; c) K. Eggers, F. W. Heinemann, M. Hennemann, T. Clark, P. Binger, U. Zenneck, *C. R. Chim.* **2010**, *13*, 1203–1212, and references therein.
[21] a) A. V. Petrov, A. A. Zagidullin, I. A. Bezkishko, M. N. Khrizanforov, K. V. Kholin, T. P. Gerasimova, K. A. Ivshin, R. P. Shekurov, S. A. Katsyuba, O. N. Kataeva, Y. H. Budnikova, V. A. Miluykov, *Dalton Trans.* **2020**, *49*, 17252–17262; b) P. Lemoine, M. Gross, P. Braunstein, F. Mathey, B. Deschamps, J. H. Nelson, *Organometallics* **1984**, *3*, 1303–1307; c) G. De Lauzon, F. Mathey, M. Simalty, *J. Organomet. Chem.* **1978**, *156*, C33-C36.
[22] a) R. Wolf, A. W. Ehlers, M. M. Khusniyarov, F. Hartl, B. de Bruin, G. J. Long, F. Grandjean, F. M. Schappacher, R. Pottgen, J. C. Slootweg, M. Lutz, A. L. Spek, K. Lammertsma, *Chem. Eur. J.* **2010**, *16*, 14322–14334; b) V. Lyaskovskyy, N. Elders, A. W. Ehlers, M. Lutz, J. C. Slootweg, K. Lammertsma, *J. Am. Chem. Soc.* **2011**, *133*, 9704–9707; c) A. Chirila, R. Wolf, J. C. Slootweg, K. Lammertsma, *Coord. Chem. Rev.* **2014**, *270–271*, 57–74; d) A. Efraty, *Chem. Rev.* **1977**, *77*, 691–744; e) Z. C. Wang, L. Qiao, Z. M. Sun, M. Scheer, *J. Am. Chem. Soc.* **2022**, *144*, 6698–6702.
[23] Z. Li, X. Chen, D. M. Andrada, G. Frenking, Z. Benko, Y. Li, J. R. Harmer, C. Y. Su, H. Grützmacher, *Angew. Chem. Int. Ed.* **2017**, *56*, 5744–5749; *Angew. Chem.* **2017**, *129*, 5838–5843.
[24] Z. Li, X. Chen, L. L. Liu, M. T. Scharnhölz, H. Grützmacher, *Angew. Chem. Int. Ed.* **2020**, *59*, 4288–4293; *Angew. Chem.* **2020**, *132*, 4318–4323.
[25] Alternatively, **2** can be oxidized with $Fc[PF_6]$ to form **3**$[PF_6]$ and reduced after loss of a CO ligand. An advantage of this procedure is the lesser solubility of $K[PF_6]$, which leads to a cleaner product.
[26] Deposition Numbers 2089380, 2089381, 2089382 and 2096257 contain the supplementary crystallographic data for this paper. These data are provided free of charge by the joint Cambridge Crystallographic Data Centre and Fachinformationszentrum Karlsruhe Access Structures service.
[27] M. E. Gress, R. A. Jacobson, *Inorg. Chem.* **1973**, *12*, 1746–1749.
[28] G. J. Long, D. G. Alway, K. W. Barnett, *Inorg. Chem.* **1978**, *17*, 486–489.
[29] E. Hey-Hawkins, H. G. von Schnering, *Z. Naturforsch. B* **1991**, *46*, 621–624.
[30] P. D. Harvey, W. P. Schaefer, H. B. Gray, D. F. R. Gilson, I. S. Butler, *Inorg. Chem.* **1988**, *27*, 57–59.
[31] R. H. Herber, R. B. King, M. N. Ackermann, *J. Am. Chem. Soc.* **1974**, *96*, 5437–5441.
[32] a) G. Jeschke, R. Rakhmatullin, A. Schweiger, *J. Magn. Reson.* **1998**, *131*, 261–271; b) P. Höfer, A. Grupp, H. Nebenführ, M. Mehring, *Chem. Phys. Lett.* **1986**, *132*, 279–282.
[33] a) P. Gütlich, E. Bill, A. X. Trautwein, *Mössbauer Spectroscopy and Transition Metal Chemistry*, Springer, Heidelberg, **2011**; b) R. L. Collins, R. Pettit, *J. Am. Chem. Soc.* **1963**, *85*, 2332–2333.
[34] a) K. Wade, *J. Chem. Soc. D* **1971**, 792–793; b) D. M. P. Mingos, *Acc. Chem. Res.* **1984**, *17*, 311–319; c) R. W. Rudolph, *Acc. Chem. Res.* **1976**, *9*, 446–452.
[35] G. Knizia, *J. Chem. Theory Comput.* **2013**, *9*, 4834–4843.
[36] G. C.-V. M. Gimferrer, P. Salvador, *Molecules* **2020**, *25*, 234.

[37] F. W. F. Neese, U. Becker, C. Riplinger, *J. Chem. Phys.* **2020**, *152*, 224108.
[38] M. Fritz, S. Schneider in *The Periodic Table II: Catalytic, Materials, Biological and Medical Applications* (Ed.: D. M. P. Mingos), Springer International Publishing, Cham, **2019**, pp. 1–36.

Manuscript received: April 27, 2022
Accepted manuscript online: June 4, 2022
Version of record online: July 11, 2022